Coral Reefs (2017) 36:269–275
DOI 10.1007/s00338-016-1522-0

NOTE

Mapping coral reefs using consumer-grade drones and structure from motion photogrammetry techniques

Elisa Casella[1] · Antoine Collin[2] · Daniel Harris[1,3] · Sebastian Ferse[1] · Sonia Bejarano[1] · Valeriano Parravicini[6,7] · James L. Hench[4] · Alessio Rovere[1,3,5]

Received: 26 June 2016 / Accepted: 17 November 2016 / Published online: 28 November 2016

Abstract We propose a novel technique to measure the small-scale three-dimensional features of a shallow-water coral reef using a small drone equipped with a consumer-grade camera, a handheld GPS and structure from motion (SfM) algorithms. We used a GoPro HERO4 with a modified lens mounted on a DJI Phantom 2 drone (maximum total take-off weight <2 kg) to perform a 10 min flight and collect 306 aerial images with an overlap equal or greater than 90%. We mapped an area of 8380 m^2, obtaining as output an ortho-rectified aerial photomosaic and a bathymetric digital elevation model (DEM) with a resolution of 0.78 and 1.56 cm $pixel^{-1}$, respectively. Through comparison with airborne LiDAR data for the same area, we verified that the location of the ortho-rectified aerial photomosaic is accurate within ~1.4 m. The bathymetric difference between our DEM and the LiDAR dataset is -0.016 ± 0.45 m (1σ). Our results show that it is possible, in conditions of calm waters, low winds and minimal sun glint, to deploy consumer-grade drones as a relatively low-cost and rapid survey technique to produce multispectral and bathymetric data on shallow-water coral reefs. We discuss the utility of such data to monitor temporal changes in topographic complexity of reefs and associated biological processes.

Keywords Drone mapping · Coral reefs · Bathymetry from drones · Structure from motion underwater · Bathymetry from photogrammetry

Communicated by Geology Editor Prof. Eberhard Gischler

Electronic supplementary material The online version of this article (doi:10.1007/s00338-016-1522-0) contains supplementary material, which is available to authorized users.

✉ Elisa Casella
elisacasellaphd@gmail.com

Alessio Rovere
http://www.coastalgeomorphology.org

1 ZMT, Leibniz Center for Tropical Marine Ecology, Bremen, Germany

2 EPHE—Ecole Pratique des Hautes Etudes, Dinard, France

3 MARUM, University of Bremen, Bremen, Germany

4 Nicholas School of the Environment, Duke University, Beaufort, NC, USA

5 Lamont Doherty Earth Observatory, Columbia University, New York, NY, USA

6 Ecole Pratique des Hautes Etudes, Paris, Sciences et Lettres Research University, Université de Perpignan, CNRS, USR 3278 Centre de Recherches Insulaires et Observatoire de l'environnement, Perpignan, France

7 Laboratoire d'Excellence, CORAIL, Perpignan, France

Introduction

Monitoring the characteristics of coral reefs is essential to understand their trajectories under scenarios of climatic or anthropogenic stress or their recovery from these impacts (Hedley et al. 2016). Large-scale studies on shallow-water coral reefs are usually carried out analysing either satellite (Mumby et al. 1997) or other airborne imagery such as aerial photographs, which are currently extensively used to monitor the trajectory of bleaching events (Normile 2016; Witze 2016). Bathymetric information on coral reefs is most often collected using echosounders or multibeam techniques (Bejarano et al. 2011), shallow-water LiDAR (Costa et al. 2009), or analysis of multispectral satellite imagery (Hedley et al. 2016).

The recent development of low-altitude airborne sensors, such as those mounted on kites or small drones (technically referred to as remotely piloted aircraft systems, RPAS), allows obtaining, at a fraction of the cost of a typical airborne survey, low-altitude imagery that can be used for environmental monitoring (Casella et al. 2014, 2016; Bryson et al. 2016; Duffy and Anderson 2016). On land, the application of structure from motion (SfM) algorithms using aerial photographs obtained with RPAS permits the construction of a digital surface model of the surveyed area. The application of RPAS to map shallow-water areas is seldom reported (Flynn and Chapra 2014; Chirayath and Earle 2016), mostly because of two main challenges. First (a condition also valid for airborne and satellite surveys), light absorption precludes the recognition of features below a critical depth threshold (depending on water turbulence and turbidity). Second, optical distortions and reflections at the air–water interface and within the water column introduce error in photograph stitching and SfM algorithms that affect the final quality of a large-scale aerial image and the associated digital surface model.

In this note, we present the results of a survey of a shallow-water reef lagoon environment using a consumer-grade drone. We timed the survey to coincide with the virtual absence of wind, low tide and optimal location of the sun in order to avoid water motion and reflections. The drone survey images were used to construct an ortho-photomosaic and a bathymetric digital elevation model (DEM). We show that, with some limitations, photogrammetry techniques applied to photographs obtained with a consumer-grade drone can be used for high-resolution mapping of shallow-water coral reefs.

Materials and methods

We used a RPAS to obtain 306 aerial photographs covering an area of 8380 m^2 of the inner lagoon of a shallow coral reef near Tiahura, in Moorea, French Polynesia (Fig. 1a). The RPAS consisted of a small drone (DJI Phantom 2, $\sim$2 kg maximum take-off weight), a remote control, a ground station (to check the route and drone performance during flight), a photo camera controlled by the pilot, and an observer. The photo camera was a GoPro HERO4 Black with a modified lens to avoid excessive distortions (see Electronic Supplementary Materials, ESM Camera used). The cost of the entire system (drone, camera and photogrammetric software) in October 2016 was $\sim$1500 €.

Take-off and landing were controlled manually from a small boat (Figs. 1b, 2f), and the flight was performed without the aid of GPS waypoints for navigation but with altitude fixed at 30 m. The horizontal speed was $\sim$1 m s^{-1}, the flight time was 10 min, the angle of the camera was set at 90° (to collect nadir photographs) and images were taken automatically every 2 s. With such a flight path and frame rate, the final overlap of the images was $\geq$90% (ESM Fig. S2).

Fig. 1 **a** Study area, the inner lagoon of Tiahura, Moorea, French Polynesia (aerial imagery from WorldView-2, DigitalGlobe). **b** Aerial view of the boat used as landing/take-off base for the drone flight. **c** Location of one ground control point (GCP) in the surveyed area; the *circle* indicates the approximate area represented in **d**. **d** Detail of **c**, example of GCP and scale bar used to georeference the image data. **e** Composite ortho-rectified photo obtained from structure from motion (SfM, see ESM Table S1). **f** Bathymetric raster obtained from SfM, with indication of GCPs ▶

We analysed the aerial photographs with the commercial software Agisoft Photoscan (http://www.agisoft.com), which uses advanced SfM and multiview stereo algorithms to construct an ortho-photomosaic and a 3D point cloud from overlapping photographs (for details on the processing steps see Casella et al. 2014, 2016 and ESM Table S1; Processing parameters section). From the point cloud, the software generates an ortho-rectified photo mosaic and an interpolated DEM using ordinary kriging. The SfM approach requires a set of points of known coordinates (i.e. ground control points, GCPs) or lines of known length (i.e. scale bars, SBs) to compute pixel-to-earth transformations and georeference the data point cloud (Fig. 1c, d).

For the SfM calculations, we inserted nine GCPs and three SBs. As targets, we used either coloured markers fixed on the bottom (Fig. 1d) or conspicuous coral heads, such as the centre of large *Porites* colonies, which could be easily identified in the aerial pictures. At each point, we measured the depth with a metered rod. We measured the position of each GCP with a handheld GPS, acquiring a fixed position for 5 min at 1 Hz frequency. This yields higher horizontal positioning accuracy than normally possible with a handheld GPS, although still in the meters range. All depths were referenced to chart datum (lowest astronomical tide, 0.34 m below mean sea level) using the time of survey and data from the nearby tidal station of Papeete (http://maree.shom.fr/).

We compared the SfM-derived bathymetric DEM with an airborne LiDAR dataset from a fixed wing aerial survey using a topobathymetric laser RIEGL VQ-820-G (June 2015), providing an average of 4 points m^{-2} with a vertical accuracy of 0.25 m and an horizontal accuracy of 1 m (ESM LiDAR data). First, we used the position of four large coral heads visible in both the LiDAR and our ortho-photomosaic to align these two datasets (ESM Fig. S1; Table S2). Second, we subtracted the elevation of each LiDAR point to the elevation of the corresponding location on the DEM to evaluate the residuals and estimate the relative vertical accuracy of our DEM against the LiDAR.

The drone survey was performed on 17 August 2015. It is worth highlighting that atmospheric and marine weather

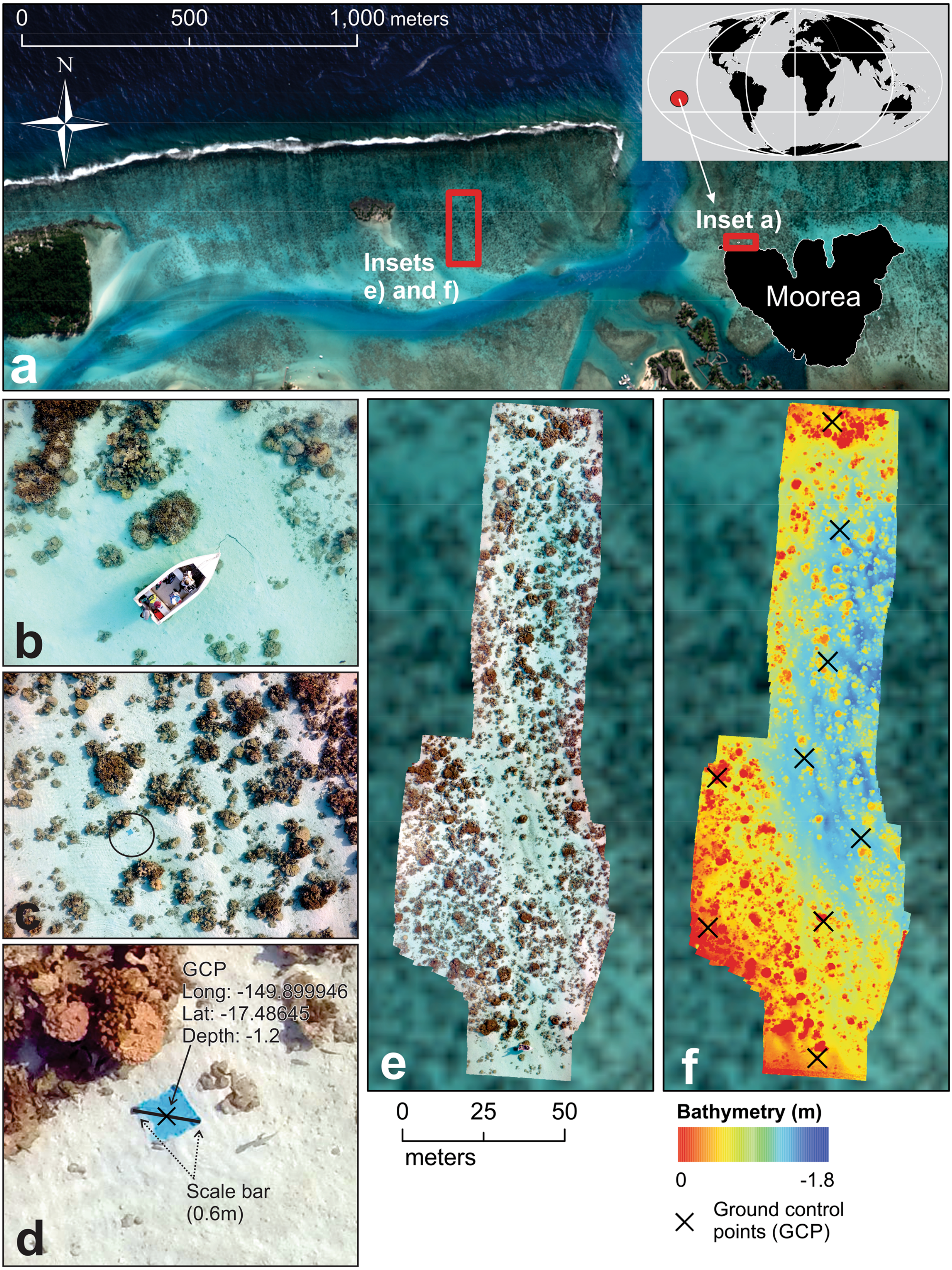
0
500
1,000 meters
N
Inset a)
Insets
e) and f)
Moorea
a
b
c
GCP
Long: -149.899946
Lat: -17.48645
Depth: -1.2
Scale bar
(0.6m)
d
e
f
0
25
50
meters
Bathymetry (m)
0
-1.8
Ground control
points (GCP)

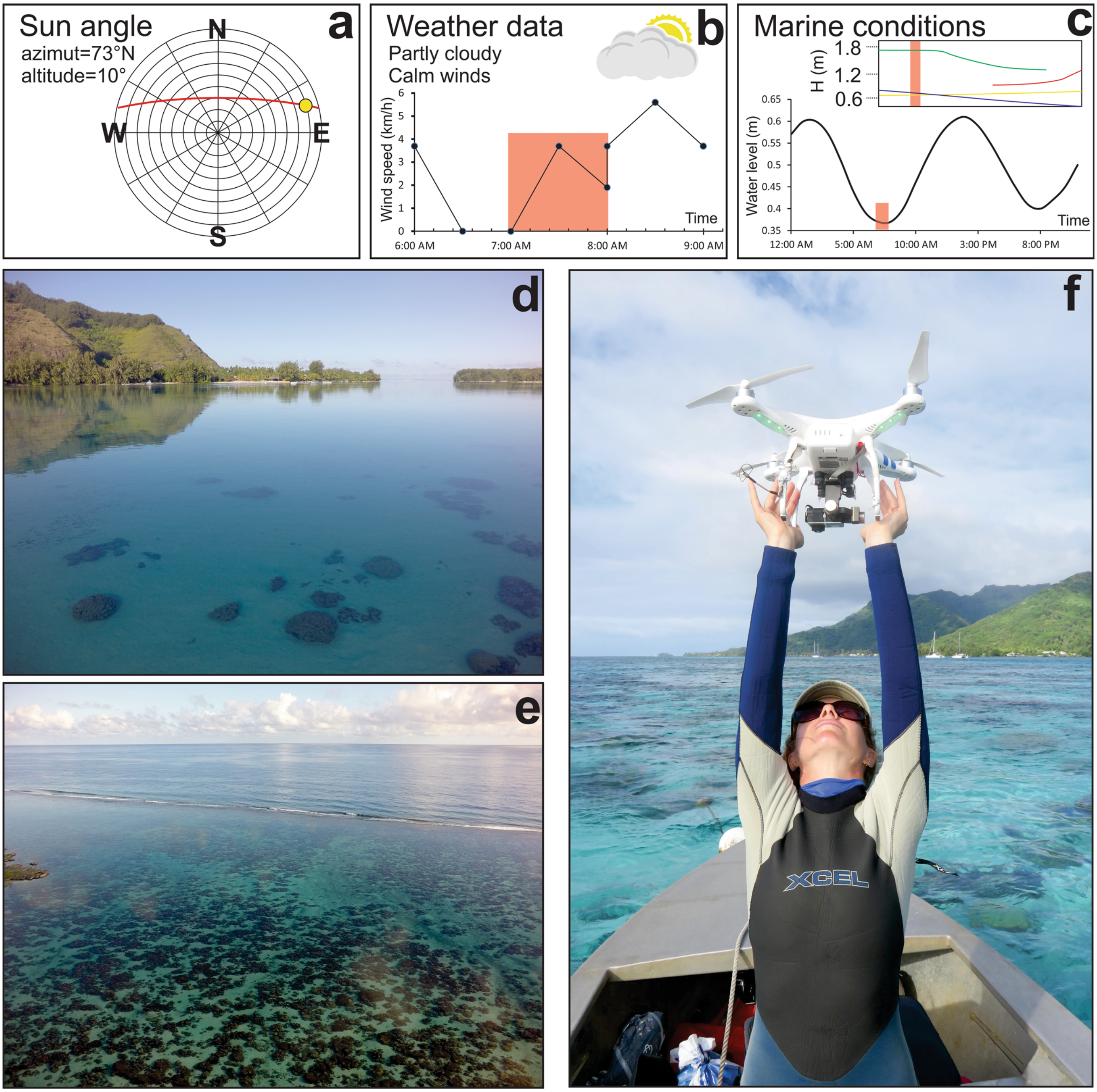

Fig. 2 **a** Sun azimuth and altitude on 17 August 2015 at 0700 h. **b** Wind and weather data (retrieved from www.wunderground.com) during the survey. **c** Tide data (http://maree.shom.fr/) and wave heights (*inset*, www.surfline.com) during the survey (*different colours* represent swells with different directions). The *red bands* in **b** and **c** represent the period of the survey. **d**, **e** Different views of the study area from oblique drone photos taken at approximately 0810 h on 17 August 2015; **f** Drone take-off from a small boat

conditions probably represent the main limitation to this method. The survey was carried out early in the morning (0700–0800 h) with calm wave conditions on the outer reef and winds of less than 2 km h^{-1} to avoid distortions on the images arising from water motion. Photographs were taken with the sun low on the horizon (Fig. 2). This helped avoid sun glint that can cause misalignments in the photogrammetric workflow.

Results and discussion

The drone imagery dataset collected in this study has an effective overlap of 30 (ESM Fig. S2). This means that each point in the sparse point cloud (first step of the SfM process) is visible or matched in an average of 30 photographs. This is a high value compared with most photogrammetric studies on land; typically, good results are

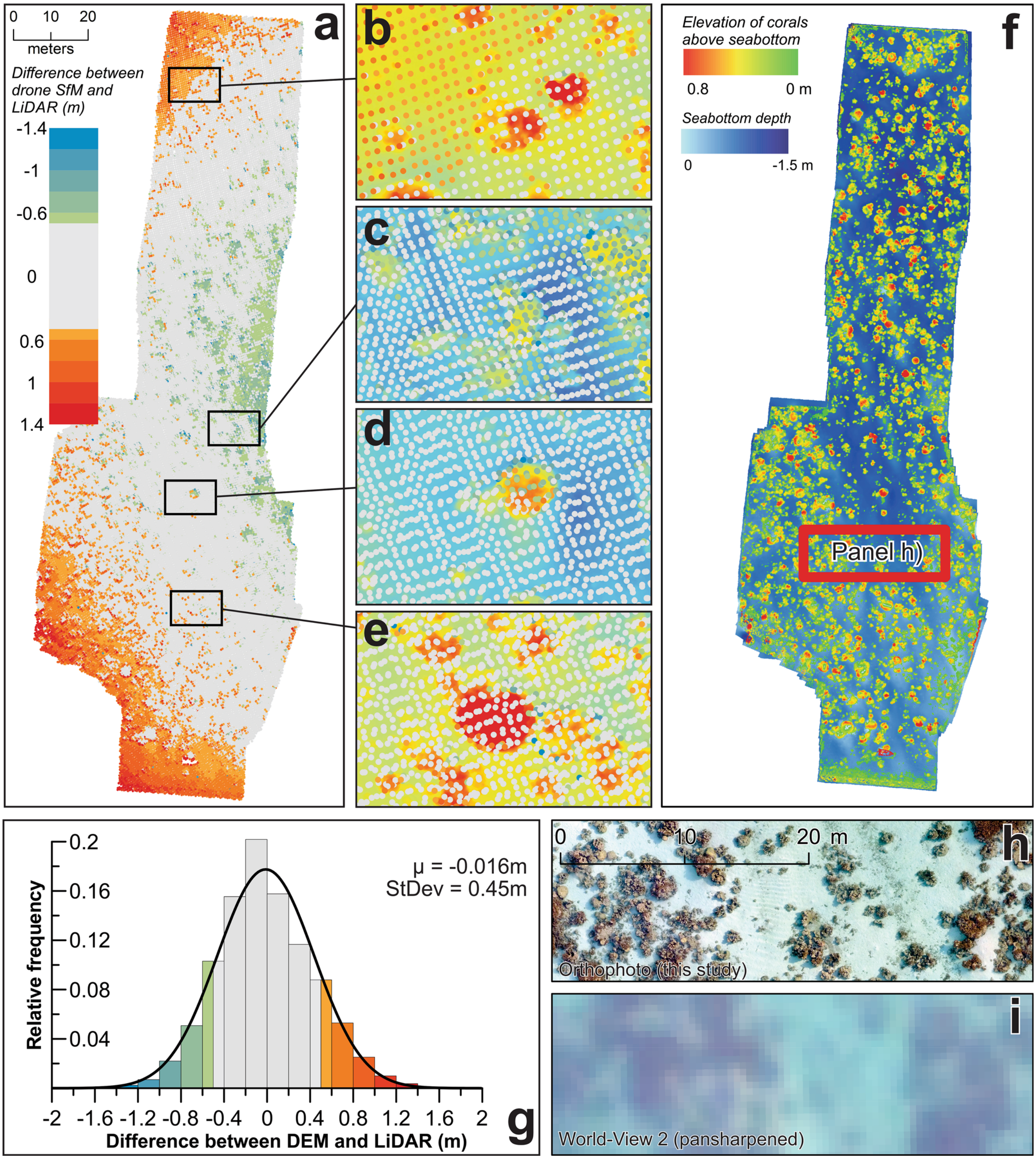

Fig. 3 **a** Difference between the depth of the DEM (drone SfM) and the LiDAR point cloud at the corresponding location. *Grey areas* correspond to areas where the difference between DEM and LiDAR falls within one standard deviation; **b–e** Detail of **a** with the DEM in Fig. 1f as the background. The *colour scale* of the DEM in the background in **b–e** is the same as in Fig. 1f. **f** Elevation of corals above the seafloor obtained by applying geometrical filtering parameters. **g** Histogram and Gaussian distribution representing the difference between DEM and LiDAR, the *colour scale* of the histograms is the same as in **a**. **h** Detail of the ortho-photomosaic obtained in this study. **i** Same area represented in pansharpened WorldView-2 imagery, DigitalGlobe (R,G,B bands)

obtained with an effective overlap of 10, depending on the type of scene. The final results of the survey are an ortho-rectified photomosaic (red, green and blue bands) and a DEM dataset in raster format, with a final ground resolution of 0.78 and 1.56 cm $pixel^{-1}$, respectively (Fig. 1e, f). The bathymetric dataset was interpolated using ordinary kriging from a dense 3D point cloud consisting of 4099 points m^{-2}. The internal consistency of the results can be constrained between 0.45 m in the horizontal and 0.16 m in the vertical plane (ESM Table S4).

The horizontal accuracy of the SfM bathymetry data can be estimated from the points used to align these data to the LiDAR point cloud. The distance between the points in our ortho-photomosaic and the equivalent points in the DEM averages to 1.4 m, which can be interpreted as a measure of positioning accuracy of our data (ESM Fig. S1; Table S2). Such positioning accuracy is rather poor, and stems from the use of a handheld GPS for the collection of GCPs.

The vertical accuracy can be instead estimated by the difference between the LiDAR point cloud and our aligned DEM (Fig. 3a–e). This difference averages at −0.016 m and has a standard deviation of 0.45 m (Fig. 3g). Note that the LiDAR itself has an accuracy of 0.25 m. From the spatial pattern of this difference (Fig. 3a), it appears that our workflow works better where pictures are taken at nadir, while the bathymetric reconstruction of peripheral areas in the scene may be affected by water refraction and, thus, present larger errors in the DEM reconstruction. In the near future, it is likely that even higher accuracies than those presented here will be obtained applying fluid lensing correction techniques, which are still experimental (Chirayath and Earle 2016). Nevertheless, we underline that the results presented here (obtained using consumer-grade survey equipment) are already usable to study different aspects of reef ecology and geomorphology.

The small-scale dataset obtained in this study can be employed in shallow-water as a first-order ground-truthing to calibrate depths derived from larger-scale optical products, such as satellite imagery (Lesser and Mobley 2007; Collin et al. 2014). The Agisoft Photoscan workflow allows obtaining bathymetric datasets in both raster and point cloud formats. The latter has the advantage of allowing geometrical filtering (ESM Table S1), and the identification of areas dominated by stony corals (Fig. 3f). This enables the calculation of volumes of corals occupying the surveyed area with classic cut/fill DEM analyses and the computation of landscape-scale rugosity measures.

The resolution of the ortho-photomosaic is high compared with the most detailed commercially available satellite imagery that is often used for coral reef mapping (e.g. WorldView-2; Fig. 3h, i). Therefore, for larger corals, it is possible to discern different genera or growth forms. Moreover, high-resolution drone surveys can be repeated frequently in time, and changes in coral cover and incidence of coral bleaching can be detected and linked to information on coral morphology. This would represent a valuable technique to monitor, over fixed aerial transects, perturbations such as coral bleaching or *Acanthaster planci* outbreaks, or grazing halos as proxies of predator removal (Madin et al. 2011).

Another key parameter that can be measured through the technique presented in this note is reef rugosity. Rugosity is a key structural variable of coral reefs. It correlates with fish density, diversity, biomass, grazing by sea urchins, reef accretion and the recovery capacity of the system after disturbance (Graham and Nash 2013; Graham et al. 2015). Moreover, rugosity positively affects the entire trophodynamics of coral reefs by providing refuges and high rates of suspension feeding in cavities (Richter and Wunsch 1999; Rogers et al. 2014). It enhances key ecosystem services such as fisheries catches (Graham 2014), nutrient cycling (Szmant 1997) and coastal protection by the dissipation of wave energy (Lugo-Fernández et al. 1998; Sheppard et al. 2005; Ferrario et al. 2014). Information on this parameter is therefore of primary importance for the study of ecosystem functioning, and the development of spatially resolved management measures (Mumby 2016).

The relevance of deriving rugosity layers with drone images spans beyond predicting patterns of fish biomass and species diversity. Concomitant with the rapid decline of hard coral cover, the complex architecture of reefs is flattening at relatively fast rates (Alvarez-Filip et al. 2011). Drone-derived rugosity offers a cost-effective alternative to monitor temporal changes in topographic complexity of reefs. Coupled with modelling approaches, drone-generated rugosity data could aid in the generation of future spatial predictions of habitat loss and fish stocks decline.

In conclusion, our results show that consumer-grade drones can be effective for applied in the monitoring of coral reefs at scales that lie between the typical scales of SCUBA or snorkelling surveys and those typical of airborne or satellite mapping (Hedley et al. 2016). If survey times are carefully planned to avoid excessive water motion and undesirable reflections, DEM bathymetry datasets obtained with consumer-grade drones have a vertical accuracy of ± 0.45 m (1σ) compared to LiDAR. Imagery and bathymetric information obtained from consumer-grade drones are therefore useful tools to obtain repeatable and low-cost data on shallow-water coral reefs, which are also the most prone to environmental stressors.

Acknowledgements This research was supported by the Institutional Strategy of the University of Bremen, funded by the German Excellence Initiative (ABPZuK-03/2014) and by ZMT, the Leibniz Center for Tropical Marine Ecology, Bremen. We acknowledge the Centre de Recherches Insulaires et Observatoire de l'Environnement

(CRIOBE) for support during the field data collection. The airborne LiDAR measurements and analysis were supported by the US National Science Foundation grants OCE1435133 (Physical Oceanography) as well as OCE1236905 and OCE1637396 (Moorea Coral Reef LTER). We acknowledge useful assessments and corrections from two anonymous reviewers as well as the journal editor.

References

Alvarez-Filip L, Gill JA, Dulvy NK, Perry AL, Watkinson AR, Côté IM (2011) Drivers of region wide declines in architectural complexity on Caribbean reefs. Coral Reefs 30:1051–1060

Bejarano S, Mumby PJ, Sotheran I (2011) Predicting structural complexity of reefs and fish abundance using acoustic remote sensing (RoxAnn). Mar Biol 158:489–504

Bryson M, Duce S, Harris D, Webster JM, Thompson A, Vila-Concejo A, Williams SB (2016) Geomorphic changes of a coral shingle cay measured using kite aerial photography. Geomorphology 270:1–8

Casella E, Rovere A, Pedroncini A, Stark CP, Casella M, Ferrari M, Firpo M (2016) Drones as tools for monitoring beach topography changes in the Ligurian Sea (NW Mediterranean). Geo-Mar Lett 36:151–163

Casella E, Rovere A, Pedroncini A, Mucerino L, Casella M, Cusati AL, Vacchi M, Ferrari M, Firpo M (2014) Study of wave runup using numerical models and low-altitude aerial photogrammetry: a tool for coastal management. Estuar Coast Shelf Sci 149:160–167

Chirayath V, Earle S (2016) Drones that see through waves—preliminary results from airborne fluid lensing for centimetre-scale aquatic conservation. Aquat Conserv 26:237–250

Collin A, Archambault P, Planes S (2014) Revealing the regime of shallow coral reefs at patch scale by continuous spatial modeling. Front Mar Sci 1:65

Costa BM, Battista TA, Pittman SJ (2009) Comparative evaluation of airborne LiDAR and ship-based multibeam SoNAR bathymetry and intensity for mapping coral reef ecosystems. Remote Sens Environ 113:1082–1100

Duffy JP, Anderson K (2016) A 21st-century renaissance of kites as platforms for proximal sensing. Prog Phys Geogr 40:352–361

Ferrario F, Beck MW, Storlazzi CD, Micheli F, Shepard CC, Airoldi L (2014) The effectiveness of coral reefs for coastal hazard risk reduction and adaptation. Nat Commun 5:3794

Flynn KF, Chapra SC (2014) Remote sensing of submerged aquatic vegetation in a shallow non-turbid river using an unmanned aerial vehicle. Remote Sens 6:12815–12836

Graham NA (2014) Habitat complexity: coral structural loss leads to fisheries declines. Curr Biol 24:R359–R361

Graham NAJ, Nash KL (2013) The importance of structural complexity in coral reef ecosystems. Coral Reefs 32:315–326

Graham NA, Jennings S, MacNeil MA, Mouillot D, Wilson SK (2015) Predicting climate-driven regime shifts versus rebound potential in coral reefs. Nature 518:94–97

Hedley J, Roelfsema C, Chollett I, Harborne A, Heron S, Weeks S, Skirving W, Strong A, Eakin C, Christensen T, Ticzon V, Bejarano S, Mumby P (2016) Remote sensing of coral reefs for monitoring and management: a review. Remote Sens 8:118

Lesser MP, Mobley CD (2007) Bathymetry, water optical properties, and benthic classification of coral reefs using hyperspectral remote sensing imagery. Coral Reefs 26:819–829

Lugo-Fernández A, Roberts HH, Suhayda JN (1998) Wave transformations across a Caribbean fringing-barrier coral reef. Cont Shelf Res 18:1099–1124

Madin EM, Madin JS, Booth DJ (2011) Landscape of fear visible from space. Sci Rep 1:14

Mumby PJ (2016) Stratifying herbivore fisheries by habitat to avoid ecosystem overfishing of coral reefs. Fish Fish 17:266–278

Mumby PJ, Green EP, Edwards AJ, Clark CD (1997) Coral reef habitat mapping: how much detail can remote sensing provide? Mar Biol 130:193–202

Normile D (2016) El Niño's warmth devastating reefs worldwide. Science 352:15–16

Richter C, Wunsch M (1999) Cavity-dwelling suspension feeders in coral reefs—a new link in reef trophodynamics. Mar Ecol Prog Ser 188:105–116

Rogers A, Blanchard JL, Mumby PJ (2014) Vulnerability of coral reef fisheries to a loss of structural complexity. Curr Biol 24:1000–1005

Sheppard C, Dixon DJ, Gourlay M, Sheppard A, Payet R (2005) Coral mortality increases wave energy reaching shores protected by reef flats: examples from the Seychelles. Estuar Coast Shelf Sci 64:223–234

Szmant AM (1997) Nutrient effects on coral reefs: a hypothesis on the importance of topographic and trophic complexity to reef nutrient dynamics. Proc 8th Int Coral Reef Symp 2:1527–1532

Witze A (2016) Marine ecologists take to the skies to study coral reefs. Nature 534:13–14